

Excitons in carbon nanotubes: an *ab initio* symmetry-based approach

Eric Chang, Giovanni Bussi, Alice Ruini, and Elisa Molinari

INFN National Center on nanoStructures and bioSystems at Surfaces (S³) and Dipartimento di Fisica, Università di Modena e Reggio Emilia, Via Campi 213/A, 41100 Modena, Italy

(Dated: October 21, 2018)

The optical absorption spectrum of the carbon (4,2) nanotube is computed using an *ab initio* many-body approach which takes into account excitonic effects. We develop a new method involving a local basis set which is symmetric with respect to the screw symmetry of the tube. Such a method has the advantages of scaling faster than plane-wave methods and allowing for a precise determination of the symmetry character of the single particle states, two-particle excitations, and selection rules. The binding energy of the lowest, optically active states is approximately 0.8 eV. The corresponding exciton wavefunctions are delocalized along the circumference of the tube and localized in the direction of the tube axis.

A wealth of extraordinary results concerning the mechanical and electrical properties of carbon nanotubes (NTs) have been reported in the last few years [1]. Until recently, however, their optical properties have not received the same attention: experimental work has often been hindered by low emission efficiency, and the interpretation has been complicated by the fact that tubes of different species and orientation are normally mixed together in the same sample, making it difficult to assign the measured spectra to a single NT species.

Very recent experiments have indicated that these limitations can be overcome. Improved optical efficiency has been obtained by isolating NTs in porous materials [2], in solution [3], or on patterned substrates [4]. It was possible to assign optical spectra to specific NTs via their characteristic vibrations in resonant Raman [5] or in near-field experiments [6]. The observation of electrically induced optical emission from a carbon NT FET [7] has paved the way for a new class of single-molecule experiments and devices. These advances therefore establish optical spectroscopies as powerful characterization tools for NTs. Nanotubes also hold great promise for novel nanoscale opto-electronic and photonic applications [7], because the optical gap of NTs spans a very large frequency range which overlaps with the range of interest in the field of telecommunications.

In spite of such fervent interest in this subject, the fundamental nature of optical excitations of NTs is not yet understood. The possible relevance of excitonic effects in these systems was pointed out in a pioneering paper by Ando [8]. In general, it is well known that the electron-hole interaction plays a crucial role in one-dimensional systems, not only in the ideal case [9], but also in realistic systems such as semiconductor quantum wires [10] or polymer chains [11] where excitons dominate the optical spectra. The binding energies are however very sensitive to the spatial extent of the single-particle wavefunctions and to the (anisotropic) dielectric screening [12]. In the case of NTs, one might expect these quantities to be sen-

sitive to size and geometry. Moreover, given the peculiar nature of the electronic states, even the smaller diameter NTs cannot be regarded as pure one-dimensional systems. It is therefore extremely difficult to estimate the actual relevance of excitonic effects without a realistic calculation of their optical excitations.

In this Letter, we present an efficient *ab initio* approach to compute the spectra, exciton energies and wavefunctions of carbon NTs. Such an approach includes the full three-dimensional dependence of the electron states and interactions. Our formalism exploits a fully symmetrized Gaussian basis set and allows us not only to reduce the system size and computation time considerably, but also to profit from the selection rules involving a new quantum number which comes into play in the symmetry characterization of the problem.

As a preliminary step, a calculation based on the density-functional theory within the local density approximation [13] is performed with a plane-wave basis, pseudopotentials and supercells [14] and the band states $\psi_{nk}(\mathbf{G})$ are calculated in Fourier space. These states are then projected onto a set of basis functions which are symmetrized sums of Gaussian orbitals centered on the atoms. The basis is constructed to be simultaneous eigenstates of the commuting operators \hat{G}_1 and \hat{G}_2 . \hat{G}_1 represents a discrete translation of the tube in the z -direction by the length of the cell T . \hat{G}_2 is the screw-symmetry operation consisting of a combined rotation and translation: a rotation by an angle of $2\pi/N$, where N is the number of hexagons in the supercell; and a translation along the z -direction by $(M/N)T$, where M depends on the geometry and size of the tube (for details see Ref. [1]). The basis functions have the form

$$\chi_{\sigma nlm}^{\mathbf{q}h}(\mathbf{r}) = \sum_{j_R=1}^N \sum_{j_T=1}^{N_{cell}} f_{\mathbf{q}}^{j_T} g_{\mathbf{q}h}^{j_R} [\hat{G}_2^{j_R} \hat{G}_1^{j_T} \phi_{nlm}(\mathbf{r} - \tau_{\sigma})]. \quad (1)$$

The functions $\{\phi_{nlm}(\mathbf{r})\}$ are Gaussians defined as $\phi_{nlm}(\mathbf{r}) = r^l \exp(-r^2/a_n^2) Y_{lm}(\hat{\mathbf{r}})$. They have been used with considerable success in similar calculations for ex-

tended systems [15]. N is the number of hexagons per unit cell. $\sigma = 1, 2$ labels one of the two inequivalent atoms in the unit cell. $f_{\mathbf{q}} = e^{2\pi i \mathbf{q}}$ and $g_{\mathbf{q}h} = e^{2\pi i (M\mathbf{q}+h)/N}$ are the eigenvalues of the operators \hat{G}_1 and \hat{G}_2 , respectively. h is a new quantum number, analogous to the azimuthal quantum number m , which ranges from 1 to N .

The quantities needed for the calculation of both the random phase approximation (RPA) dielectric function [16] and the Bethe Salpeter equation (BSE) matrix [17, 18, 19] are the Gaussian transition elements $A_{\gamma}^{nk,n'k'} \equiv \langle nk | \chi_{\gamma}^{k-k',h_d} | n'k' \rangle$. They are given by

$$A_{\gamma}^{nk,n'k'} = \sum_{\alpha\beta} (\psi_{nk}^{\alpha})^* \psi_{n'k'}^{\beta} M_{\alpha\gamma\beta}^{kh;k-k',h_d;k'h'}, \quad (2)$$

where ψ_{nk}^{α} is the Gaussian component of the wavefunctions of the system [Greek letters $\alpha, \beta, \gamma, \dots$ denote the quartuple (σ, n, l, m)], and $h_d = h(nk) - h(n'k')$ is the difference between the quantum number h for the states nk and $n'k'$. The three-basis-function integrals $M_{\alpha\gamma\beta}^{kh;k-k',h_d;k'h'}$ are given by :

$$M_{\alpha\gamma\beta}^{kh;k-k',h_d;k'h'} = \sum_{ii'jj'} L_{\alpha\gamma\beta}^{ij;i'j'} f_{k-k'}^i f_{k'}^{i'} g_{k-k',h_d}^j g_{k'h'}^{j'}. \quad (3)$$

The phase-multiplied three-center integrals $L_{\alpha\gamma\beta}^{ij;i'j'}$ are calculated from the pure three-center integrals $I_{ACB}^{\mathbf{R}\mathbf{R}'\mathbf{R}''} = \int d^3r \phi_A^*(\mathbf{r}-\mathbf{R}) \phi_C(\mathbf{r}-\mathbf{R}') \phi_B(\mathbf{r}-\mathbf{R}'')$ with $L_{\alpha\gamma\beta}^{ij;i'j'} = k_{m(c)}^j k_{m(b)}^{j'} I_{ACB}^{\tau;G_2^j G_1^i \tau'';G_2^{j'} G_1^{i'} \tau'}$ where $k_m = e^{-2\pi i m/N}$. $\tau, \tau',$ and τ'' are the basis vectors (atomic positions in the reduced cell) for Gaussians $\alpha, \beta,$ and γ .

The evaluation of the Gaussian transition elements and the three-basis-function integrals in Eq. (2) and Eq. (3) is the most expensive part of the calculation and, for a given precision, scales like $\sim (NN_k)^2 \sim R^2$, where N_k is the number of k -points and R is the radius of the tube. This scaling is considerably faster than that of a plane-wave calculation, which scales like $\sim TR^4 \log(TR^2)$. Our method has the additional advantage of scaling independently of the cell length T and allows for a calculation of tubes like the (4,2) NT, which have unusually long cell lengths.

The expressions for the BSE matrix are simple functions of the matrix elements in Eq. (2). We distinguish two cases: (a) If the light is polarized along the tube axis, z , the selection rule for h is $h = h'$. For this polarization we include only those transitions which conserve h . In so doing, the BSE matrix is reduced to N independent blocks. (b) The same holds for circularly-polarized light with polarization vector $\hat{\mathbf{e}}_{\pm} = 1/\sqrt{2}(\hat{\mathbf{e}}_x \pm i\hat{\mathbf{e}}_y)$ with the only difference that the selection rule is $h = h' \pm 1$. The direct term for both polarizations is:

$$K_{cvk,c'v'k'}^d = A_{\alpha}^{ck,c'k'} [A_{\beta}^{vk,v'k'}]^* W_{k-k',h(ck)-h(c'k')}^{\alpha\beta}. \quad (4)$$

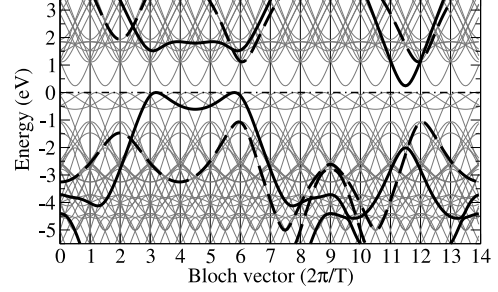


FIG. 1: Band structure in the extended zone scheme. Each panel represents a full Brillouin zone (FBZ). The solid line represents a continuation of a band with character $h = 1$ in the first Brillouin zone, and the dashed line begins with a band with character $h = 2$. The top of the valence band is represent by a horizontal dotted-dashed line.

The exchange term is:

$$K_{cvk,c'v'k'}^x = A_{\alpha}^{ck,vk} [A_{\beta}^{c'k',v'k'}]^* V_{0,h(ck)-h(vk)}^{\alpha\beta}, \quad (5)$$

where $h(ck) - h(vk) = 0 (\pm 1)$ for the $\hat{\mathbf{e}}_z$ ($\hat{\mathbf{e}}_{\pm}$) polarization, $W_{q,h}^{\alpha\beta}$ and $V_{q,h}^{\alpha\beta}$ are the screened and bare Coulomb interactions expressed in the symmetrized basis of Gaussians (the Einstein sum convention is used to sum over the Greek indices) calculated following the procedure in Ref. [15]. The screening is calculated in RPA. Building the matrices in Eq. (4) and Eq. (5) does not require much computation time because the Greek indices range from 1 to the number of Gaussians (fifty in this work) which is small and does not depend on system size.

The exciton wavefunction for the n^{th} excitation is:

$$\phi^{(n)}(\mathbf{r}_e, \mathbf{r}_h) = \sum_{cvk} \Psi_{cvk}^{(n)} [\psi_{vk}(\mathbf{r}_h)]^* \psi_{ck}(\mathbf{r}_e), \quad (6)$$

where the expansion coefficients $\Psi_{cvk}^{(n)}$ satisfy the BSE:

$$[(E_{ck} - E_{vk}) \delta_{cc'} \delta_{vv'} \delta_{kk'} + K_{cvk,c'v'k'}] \Psi_{c'v'k'}^{(n)} = \Omega_n \Psi_{cvk}^{(n)}, \quad (7)$$

with $K_{cvk,c'v'k'} = 2K_{cvk,c'v'k'}^x - K_{cvk,c'v'k'}^d$. Since we are interested only in the effect of the electron-hole interaction on the spectra, we use LDA energies for the E_{nk} of Eq. 7 without quasiparticle corrections [20]. The imaginary part of the dielectric function is given by $\epsilon_2(\omega) = 4\pi/\omega^2 \sum_n |M_n|^2 \delta(\omega - \Omega_n)$ where $M_n = \sum_{cvk} \Psi_{cvk}^{(n)} \langle v\mathbf{k} | \mathbf{v} \cdot \mathbf{e} | c\mathbf{k} \rangle$. In this work, the momentum operator is used in lieu of the velocity operator since the former is easier to express in Gaussians. The difference in another carbon-based system, i.e., diamond, has been

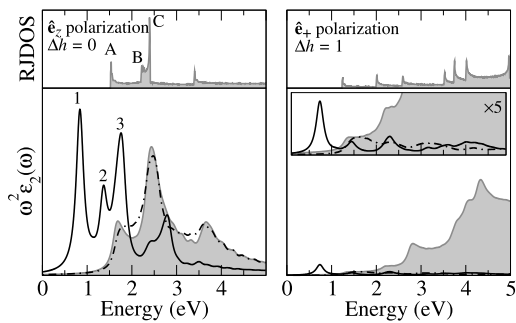


FIG. 2: The left panels show the RJDOS and the optical absorption for the \hat{e}_z polarization and the right panels for the \hat{e}_+ polarization. In both bottom panels, the solid line represents the spectrum with electron-hole interaction and the light grey line the spectrum in the single-particle picture. The dotted-dashed line represents the spectrum with exchange term only. All spectra are computed with a broadening of 0.07 eV, without self-energy corrections.

shown to be a 15 % to 20 % effect in the peak intensity of absorption spectrum [21], but has a negligible effect on the peak position.

We focus on the carbon (4,2) NT [22]. Fig. 1 shows its electronic band structure. It is represented in the extended zone scheme to clearly show how the bands unfold and how they are related to the quantum numbers h and \mathbf{k} . Every panel corresponds to a FBZ. The entire band structure is shown with light grey lines. The thick solid (dashed) lines are lines of constant character $h = 1$ ($h = 2$). In this scheme, it is clear how to represent the set of all optically permitted transitions for both polarizations (\hat{e}_z and \hat{e}_\pm). For the \hat{e}_z polarization, only the vertical transitions from the solid valence line to the solid conduction line and those from the dashed valence line to the dashed conduction line are optically allowed. For the \hat{e}_\pm polarization, only the vertical transitions from the solid to dashed line, or viceversa, depending on the helicity of the polarization, are optically allowed. Due to symmetry, both helicities (\hat{e}_+ and \hat{e}_-) yield the same spectrum. In the non-interacting theory, these transitions can be represented using a reduced joint density of states (RJDOS). It is obtained by excluding from the joint density of states all optical transitions forbidden by symmetry. The RJDOS for both polarizations is shown in the top two panels of Fig. 2. The corresponding absorption spectra are shown in the bottom two panels. They are computed with 24 k-points in the FBZ and a broadening of 0.07 eV. The BSE matrix computed with this k-point sampling and for the energy range of inter-

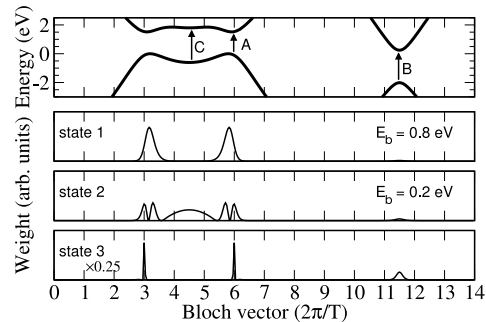


FIG. 3: The top panel shows a portion of the band structure in the extended zone scheme with the relevant bands [solid bold line ($h = 1$) in Fig. 1]. The bottom three panels show the weighted contributions of the transitions which comprise three excitonic states that correspond to the first three peaks in the absorption spectrum for the \hat{e}_z polarization.

est is small with dimension $\approx 300 \times 300$. For the \hat{e}_z polarization, the absorption spectrum with excitonic effects (solid line of bottom left panel of Fig. 2) has three peaks: the lowest two peaks correspond to bound excitons with binding energies $E_b = 0.8$ eV and $E_b = 0.2$ eV, while the third one is an unbound resonance. This is consistent with the value of 1.0 eV found for an (8,0) nanotube in another work [23].

To gain a better understanding of the nature of the excitonic states giving rise to these three peaks, we consider the three corresponding excitonic states with the highest oscillator strength M_n . Fig. 3 shows, in the extended zone scheme, the weighted contributions of the optical transitions to these states (bottom three panels). State 1 is made up of transition A shown in the band diagram (top panel). State 2 is derived from transitions A and C, and state 3 from transitions A and B. Transitions A, B, and C correspond to the Van Hove singularities in the RJDOS labeled in the top left panel of Fig. 2. Note that the resonance represented by state 3 is coupled with transitions in the continuum region, appearing in Fig. 3 (bottom panel) as two sharp peaks each corresponding to a single Bloch vector.

From the bottom left panel of Fig. 2 one can directly compare the absorption with both direct and exchange terms included in the BSE (solid line), the absorption with exchange term only (dotted-dashed lines), and the absorption without excitonic effects (the shaded line): it is evident that excitonic effects radically alter the absorption spectrum. Moreover, most of the effect comes from the direct term, as the exchange term alters the spectrum by a small amount.

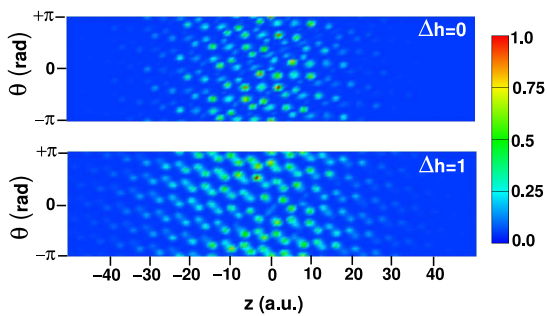


FIG. 4: Exciton wavefunctions for the two lowest, optically active excitons of the (4,2) carbon NT. The top panel shows the $\Delta h = 0$ exciton ($E_b = 0.8$ eV) and the bottom panel the $\Delta h = 1$ exciton ($E_b = 0.6$ eV). The color plots represent the projection on the tube lateral surface of the probability of finding the hole when the electron is fixed in the origin slightly above one of the atoms. z is the tube axis. θ is the circumference direction.

In the bottom right panel of Fig. 2, we represent the absorption spectrum for the \hat{e}_+ polarization: the spectrum calculated using the non-interacting theory is greatly suppressed when both exchange and direct terms are included in the BSE Hamiltonian. This phenomenon was discovered in another theoretical work on nanotubes [24] using time-dependent local density approximation [25]. To see if such a suppression is to be attributed to the exchange term [equivalent to local field effects (LFE)], or to the direct electron-hole Coulomb attraction, we plot an additional curve with the exchange term only (dotted-dashed line). Fig. 2 shows that the suppression is largely due to the exchange term and that the direct term affects the spectrum less, in agreement with Ref. [24]. The main effect of the direct term is to open up a significant peak below the lowest van Hove singularity, corresponding to a bound, $\Delta h = 1$ exciton with binding energy $E_b = 0.6$ eV.

We plot the exciton wavefunction $\phi^{(n)}(\mathbf{r}_e, \mathbf{r}_h)$ [see Eq. (6)] by fixing the position of the electron: Fig. 4 shows the two lowest lying, optically active excitons for the \hat{e}_z ($\Delta h = 0$) and the \hat{e}_+ polarization ($\Delta h = 1$). Both excitons are localized in the direction of the tube axis, z , but delocalized along the tube circumference, θ . This behavior is in agreement with the variational calculation of Ref. [26]. The wavefunction for the even parity (and hence, optically inactive), $\Delta h = 0$ exciton located 0.1 eV below the first absorption peak (not shown) is similar to the lowest optically active (odd parity) exciton.

In conclusion, we have developed an efficient method for performing BSE calculations on NTs of all sizes and chiralities that uses a local, symmetry-based approach. Applying this method to a (4,2) NT, we have shown that excitonic effects are important and have quantitatively determined these effects. For the \hat{e}_z polarization ($\Delta h = 0$), the excitonic effects give rise to three enhanced

peaks, and the lowest excitation is 0.8 eV below the onset of the single-particle continuum. The corresponding exciton is localized along \hat{e}_z , but delocalized along the tube circumference. For the \hat{e}_+ polarization ($\Delta h = 1$), the exchange part of the BSE matrix drastically suppresses the absorption spectrum. The direct part opens up a large peak 0.6 eV below the single-particle singularity corresponding to a bound, localized exciton.

We are grateful to G. Goldoni, J. Menendez, and M. Rohlfing for fruitful discussion. Computer time was partly provided by CINECA through INFM Parallel Computing Projects. The support by the RTN EU Contract “EXCITING” No. HPRN-CT-2002-00317, and by FIRB “NOMADE” is also acknowledged.

-
- [1] R. Saito and G. Dresselhaus and M. S. Dresselhaus, *Physical Properties of Carbon Nanotubes* (Imperial College Press, 1999).
 - [2] Z. M. Li, Z.K.Tang, H. J. Liu, N. Wang, C. T. Chan, R. Saito, S. Okada, G. D. Li, J. S. Chen, N. Nagasawa, and S. Tsuda, *Phys. Rev. Lett.* **87**, 127401 (2001).
 - [3] M. O’Connell, S. Bachilo, C. Huffman, V. Moore, M. Strano, E. Harotz, K. Rialon, P. Boul, W. Noon, C. Kittrell, J. Ma, R. Hauge, R. Weisman, and R. Smalley, *Science* **297**, 593 (2003).
 - [4] J. Lefebvre, Y. Homma, and P. Finnie, *Phys. Rev. Lett.* **90**, 217401 (2003).
 - [5] S. M. Bachilo, M. S. Strano, C. Kittrell, R. H. Hauge, R. E. Smalley, and R. Weisman, *Science* **298**, 2361 (2002).
 - [6] A. Hartschuh, E. J. Sanchez, X. S. Xie, and L. Novotny, *Phys. Rev. Lett.* **90**, 095503 (2003).
 - [7] J. Misewich, R. Martel, P. Avouris, J. Tsang, S. Heinze, and J. Tersoff, *Science* **300**, 783 (2003).
 - [8] T. Ando, *J. Phys. Soc. of Japan* **65**, 1066 (1997).
 - [9] R. Loudon, *Am. J. Phys.* **27**, 649 (1959).
 - [10] F. Rossi and E. Molinari, *Phys. Rev. Lett.* **76**, 3642 (1996).
 - [11] A. Ruini, M. J. Caldas, G. Bussi, and E. Molinari, *Phys. Rev. Lett.* **88**, 206403 (2002).
 - [12] Typical values of exciton binding energies are of the order of 0.01-0.1 eV in semiconductor wires [10] and 0.1-1 eV in polymers [11].
 - [13] W. Kohn and L. J. Sham, *Phys. Rev.* **140**, A1133 (1965).
 - [14] S. Baroni, A. Dal Corso, S. de Gironcoli, and P. Gianozzi, 2001, <http://www.pwscf.org>.
 - [15] M. Rohlfing, P. Krüger, and J. Pollmann, *Phys. Rev. B* **52**, 1905 (1995).
 - [16] S. L. Adler, *Phys. Rev.* **126**, 413 (1962).
 - [17] L. X. Benedict, E. L. Shirley, and R. B. Bohn, *Phys. Rev. Lett.* **80**, 4514 (1998).
 - [18] S. Albrecht, L. Reining, R. Del Sole, and G. Onida, *Phys. Rev. Lett.* **80**, 4510 (1998).
 - [19] M. Rohlfing and S. G. Louie, *Phys. Rev. Lett.* **81**, 2312 (1998).
 - [20] We have calculated the self energy. The quasiparticle correction increases the valence band width by 17 %, decreasing in turn E_b by only 0.03 eV.
 - [21] S. Ismail-Beigi, E. K. Chang, and S. G. Louie,

- Phys. Rev. Lett. **87**, 087402 (2001).
- [22] In this work, we have used a cylindrical, unrelaxed structure with a C-C bond length of 1.42 Å.
- [23] C. D. Spataru, S. Ismail-Beigi, L. X. Benedict, and S. G. Louie, Phys. Rev. Lett. **92**, 077402 (2004).
- [24] A. G. Marinopoulos, L. Reining, A. Rubio, and N. Vast, Phys. Rev. Lett. **91**, 046402 (2003).
- [25] M. Petersilka, U. J. Gossmann, and E. K. U. Gross, Phys. Rev. Lett. **76**, 1212 (1996).
- [26] T. G. Pedersen, Phys. Rev. B **67**, 073401 (2003).